ChinaXiv合作期刊

Effects of restoration modes on the spatial distribution of soil physical properties after land consolidation: a multifractal analysis

KE Zengming[1], LIU Xiaoli[2], MA Lihui[1,3*], TU Wen[2], FENG Zhe[2], JIAO Feng[1,3], WANG Zhanli[1,3]

[1] State Key Laboratory of Soil Erosion and Dryland Farming on the Loess Plateau, Institute of Soil and Water Conservation, Northwest A&F University, Yangling 712100, China;
[2] College of Water Resources and Architectural Engineering, Northwest A&F University, Yangling 712100, China;
[3] Institute of Water Saving Agriculture in Arid Areas of China, Northwest A&F University, Yangling 712100, China

chinaXiv:202201.00026v1

Abstract: soil physical properties (SPP) are considered to be important indices that reflect soil structure, hydrological conditions and soil quality. It is of substantial interest to study the spatial distribution of SPP owing to the high spatial variability caused by land consolidation under various land restoration modes in excavated farmland in the loess hilly area of China. In our study, three land restoration modes were selected including natural restoration land (NR), alfalfa land (AL) and maize land (ML). Soil texture composition, including the contents of clay, silt and sand, field capacity (FC), saturated conductivity (K_s) and bulk density (BD) were determined using a multifractal analysis. SPP were found to possess variable characteristics, although land consolidation destroyed the soil structure and decreased the spatial autocorrelation. Furthermore, SPP varied with land restoration and could be illustrated by the multifractal parameters of D_1, ΔD, Δa and Δf in different modes of land restoration. Owing to multiple compaction from large machinery in the surface soil, soil particles were fine-grained and increased the spatial variability in soil texture composition under all the land restoration modes. Plough numbers and vegetative root characteristics had the most significant impacts on the improvement in SPP, which resulted in the best spatial distribution characteristics of SPP found in ML compared with those in AL and NR. In addition, compared with ML, Δa values of NR and AL were 4.9- and 3.0-fold that of FC, respectively, and Δa values of NR and AL were 2.3- and 1.5-fold higher than those of K_s, respectively. These results indicate that SPP can be rapidly improved by increasing plough numbers and planting vegetation types after land consolidation. Thus, we conclude that ML is an optimal land restoration mode that results in favorable conditions to rapidly improve SPP.

Keywords: land consolidation; land restoration; multifractal analysis; spatial distribution; soil physical properties

1 Introduction

Land consolidation is widespread throughout the world. Its goal is to provide a broad area of cultivation, improve the soil quality and production and ameliorate the ecological environment (Altes and Sang, 2011; Ying et al., 2020). There is an urgent need to consolidate the land in the

*Corresponding author: MA Lihui (E-mail: gjzmlh@126.com)
Received 2021-10-10; revised 2021-12-06; accepted 2021-12-21
© Xinjiang Institute of Ecology and Geography, Chinese Academy of Sciences, Science Press and Springer-Verlag GmbH Germany, part of Springer Nature 2021

ChinaXiv合作期刊

Loess Plateau in China, because this work is closely related to land development, agricultural production, soil desertification and flood control in the area of Yellow River (Zhu, 1995).

A land consolidation project known as "Gullies Reclamation for Farmland" was implemented in the loess hilly area of China in 2013 (Ma et al., 2020). We designated the farmland formed after land consolidation as the excavated farmland, which is a large area of flat land formed by the large-scale mechanical excavation of slope soil landfill gully, after many times of compactions (Fig. 1). Land consolidation can easily cause spatial variability in soil physical properties (SPP) (Chen et al., 2015; Chen et al., 2019). The excavated slope soil has different soil textures owing to different ages of loess formation (Li et al., 2018), and the soil texture is unevenly distributed by random landfill. In addition, the filling of gullies with depths of several tens of meters may cause the groundwater level to deepen and uneven landfill and compaction lead to uneven soil bulk density (BD) and many void pores. These factors drastically affect the ability of water to infiltrate the soil and affect the field water holding capacity and even have extreme effects on the hydrological characteristics of the soil, including the surface water, groundwater and soil water (Tripathi et al., 2009; Marschalko et al., 2012; Ren et al., 2016). Moreover, an uneven SPP will cause spatial variation on water and nutrient storage capacity and even destroy agricultural ecosystems (Liang and Wei, 2020), which will seriously affect agronomic management of the fields.

Studies have shown that land restoration can ameliorate SPP (Abed et al., 2020; Donovan and Monaghan, 2021; Wang et al., 2021), including a reduction in the rate of soil disintegration and BD (Wang et al., 2017), an increase in the soil moisture content (Fu et al., 2020), and enhanced conductivity of the saturated water and the field water holding capacity (Li et al., 2017; Wang et al., 2017; Mehdi et al., 2019; Lozano-Baez et al., 2019). In addition, Perring et al. (2012) showed that the restoration of agricultural land can benefit the ecosystem in multiple manners. To this end, three land restoration modes that included natural restoration (NR), alfalfa (*Medicago sativa* Linn) land (AL) and maize (*Zea mays* L.) land (ML) were implemented in excavated farmland (Fig. 2). Based on natural restoration of abandoned farmland in the Loess Plateau, SPP directly related to the vegetation recovery stages and the time of abandonment. Rate of improvement of the physical property of 0–20 cm soil layer is significantly higher than that of 20–40 cm soil layer (Li and Shao, 2006). Dong et al. (2016) reported that there was no considerable variation in the soil properties between AL and common farmland 10 years ago. However, after 10 years, the soil water holding capacity and water stability were significantly higher than that of common farmland, indicating that AL improved soil environment more favorably. It is apparent that the types of vegetation and tillage years have various effects on SPP. Therefore, we assumed that there are some variations in the spatial distribution of SPP under different land restoration modes in the excavated farmland.

To obtain the spatial variability of SPP, many researchers interpret spatiotemporal distributions at different scales and use appropriate research methods for data processing (Paterson et al., 2018; Li et al., 2019; Mojtaba et al., 2019). Classical statistics describe the level of variations of SPP using a coefficient of variation, but this method seriously ignores the relative position between variables. Geostatistics can effectively explain the spatiotemporal autocorrelation of variables using a semi-variant function and Kriging, but it is difficult to characterize the spatial variation (Premo, 2004). Traditional methods have an advantage since they use simple and independent analyses, but practically there are several complicated parameters that are not fully independent (Jing et al., 2019). Fractal theory based on independent correlation of variables is widely used in soil sciences, meteorology and information sciences to solve various complicated problems at the micro and macro levels (Morató et al., 2017; Paterson et al., 2018; Wang et al., 2018; Gao et al., 2021; Stanić et al., 2021; Wu et al., 2021). Qi et al. (2018) and Xia et al. (2020) reported that the spatial distribution difference of soil texture under different vegetation types can be effectively characterized using multifractal theory. Jing et al. (2019) showed that BD, saturated water conductivity and water holding capacity, all have good multifractal characteristics in farmland. Therefore, multifractal theory is an appropriate choice to evaluate the spatial variability of SPP.

The spatial distribution of SPP not only determines the soil water, fertilizer, gas and heat, but

chinaXiv:202201.00026v1

ChinaXiv合作期刊

chinaXiv:202201.00026v1

also affects the availability and supply of plant nutrients in the soil (Drewry, 2006). Therefore, it is considered to be an important index to reflect soil structure and hydrological conditions, and to evaluate soil quality (Doran et al., 1996; Boix-Fayos et al., 2001). However, there are still gaps in the study of spatial distribution of SPP under different land restoration modes in the excavated farmland due to sustainable land consolidation. Consequently, the purposes of this study are (1) to characterize the spatial variability of SPP using multifractal analysis in the excavated farmland; and (2) to discuss the mechanism of the influence of different land restoration modes on SPP.

2 Materials and methods

2.1 Study area

The study area is located in an alluvial farmland of loess hilly region in China (40°14′11″N –42°27′42″N, 75°33′16″E–80°59′7″E; Fig. 1). The region has a semi-arid continental monsoon climate with a mean annual precipitation of 505 mm and mean annual potential evaporation of 1463 mm (Ke et al., 2021).

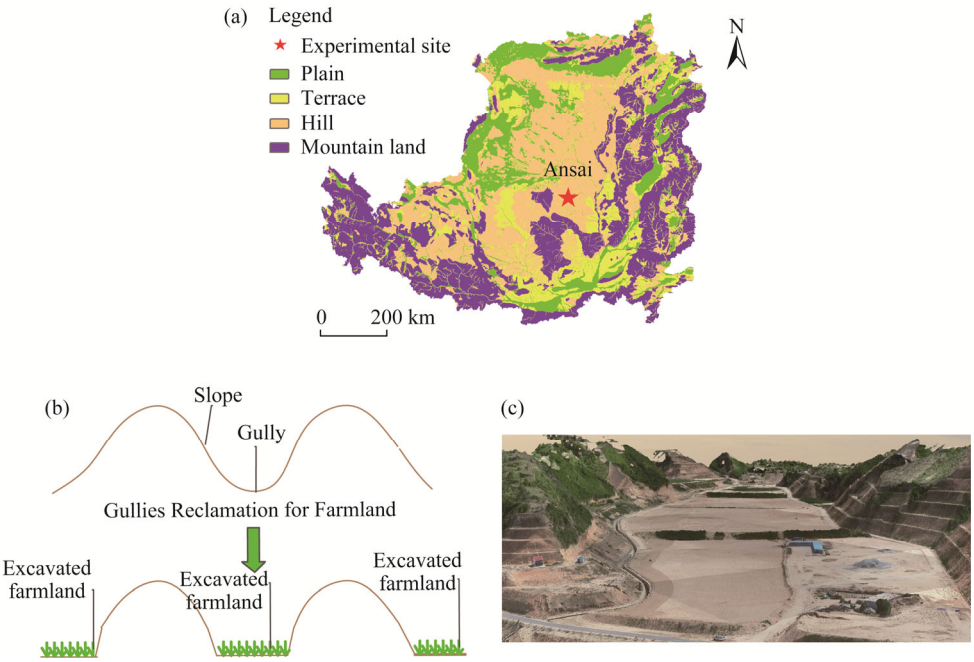

Fig. 1 (a), location of Ansai District in the hilly loess region of China; (b), schematic illustration of the "Gullies Reclamation for Farmland" project; (c), excavated farmland.

For this study, data were collected from three land restoration modes that included NR, AL and ML in the excavated farmland (Fig. 2). The topography of NR, AL and ML was similar. Moreover, one NR, one AL and one ML plot were selected and all the plots were restored after 5 years. The plot sizes were kept the same, i.e., 60 m×60 m.

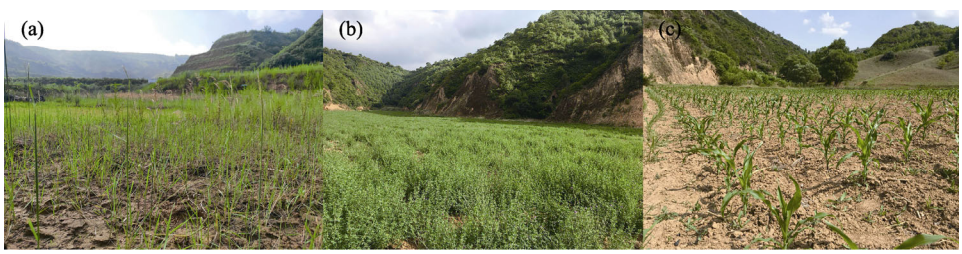

Fig. 2 Overview of study area. (a), natural restoration land; (b), alfalfa land; (c), maize land.

ChinaXiv合作期刊

2.2 Agronomic management

NR was undisturbed, and its vegetation type is mostly annual herbaceous plants. AL was five-year-old alfalfa. The forage was harvested at three times a year and ploughed once a year before returning to green. ML was planted to a season of spring maize, which was ploughed and weeded twice during the growth season, and total 600 kg P_2O_5/hm^2 (diammonium phosphate) and 100 kg N/hm^2 (urea) were applied as base fertilizer.

2.3 Sample collection and measurement

A sampling network along with squared grids (15 m×15 m) was constructed in each 0.36 hm^2 plot. NR, AL and ML plots consisted of 48 sampling points. Each sampling point was located at the individual grid center. Soil profiles were carried out in July 2018. Trimble GeoXT GPS equipment (Sunnyvale, CA, USA) with a positioning precision <0.5 m was used to locate the sampling center point coordinates. Soil texture (clay, silt and sand content), BD, saturated hydraulic conductivity (K_s) and field capacity (FC) were measured in 0–20 cm and 20–40 cm soil layers. At each sampling point, undisturbed soil samples were analyzed for their BD, FC and K_s using a ring knife (100 cm^3). To examine the soil particle size distribution (PSD), we first removed the roots and impurities in air-dried soil samples and passed through a 2-mm screen, before adding a solution of 10% H_2O_2 to degrade any organic matter. Then 0.3 g of soil was employed for laser diffraction analysis (Mastersizer 2000, Malvern Company, UK). BD and FC were evaluated using cutting ring knife method (Federer, 1983; Prévost, 2004). K_s was evaluated by a constant elevation head permeameter (TST-55, Beijing Aerospace Huayu Test Instrument Co., Ltd., Beijing, China) (Li and Shao, 2006).

2.4 Calculation of multifractal parameters

In this study, spatial variability of SPP was evaluated by multifractal analysis. A grid square with size ε, enclosed by a part of space that has SPP. These parameters were selected to identify singularity exponent $\alpha(q)$, generalized dimension $D(q)$ and singularity spectrum $f(\alpha)$ (Jing et al., 2019). In each plot, there were $N(\varepsilon)=2^k$ (k=0, 1, 2, ...) cells that were chosen (Caniego et al., 2005; Morató et al., 2017). Here in this paper, a scale of 60 m×60 m was used for each sampling plot while a scale of 15 m×15 m was used as a sampling point size. In this work, we considered four grid sizes (15, 20, 30 and 60 m) with a total number of grids, i.e., 16, 9, 4 and 1 in each plot accordingly.

A measure was defined with respect to the underlying steps to conduct a multifractal analysis. First, $P_i(\varepsilon)$ named the probability mass function was calculated as follows:

$$P_i(\varepsilon)=\frac{Z_i}{\sum_{i=1}^{N(\varepsilon)}Z_i}, \tag{1}$$

where Z_i is the value of the measure in a given size ε, and $N(\varepsilon)$ is the number of grids.

Secondly, generalized fractal dimension (D_q) is defined as follows:

$$D_q=\lim_{\varepsilon\to 0}\frac{1}{q-1}\times\frac{\lg\left(\sum_{i=1}^{N(\varepsilon)}P_i(\varepsilon)^q\right)}{\lg\varepsilon} \quad (q\neq 1), \tag{2}$$

$$D_1=\lim_{\varepsilon\to 0}\times\frac{\sum_{i=1}^{N(\varepsilon)}P_i(\varepsilon)\lg P_i(\varepsilon)}{\lg\varepsilon} \quad (q=1), \tag{3}$$

where q is the integer in (+∞, −∞), i.e., the probability density weight index (Li et al., 2011). In this study, generalized fractal dimensions D_q of reconstructed SPP were calculated for $-10\leq q\leq 10$ with increment of 1. D_1 is the information dimension. A relatively lower value of D_1 showed that the value of SPP was distributed over a relatively larger domain, owning relatively higher spatial variability, while a relatively higher value of D_1 showed that the value of SPP was focused on a relatively smaller domain, owning relatively lower value of spatial variability (Evertsz and Mandelbrot, 1992; Jing et al., 2019). ΔD, D_{-10}–D_{10}, can evaluate the intensity of spatial variability of SPP in a local distribution. ΔD value is directly correlated with variability (Zhou et al., 2010).

chinaXiv:202201.00026v1

ChinaXiv合作期刊

Thirdly, measure's multifractal spectrum, $f(q)$, can express the results. The following Legendre transformation defines $f(q)$:

$$\alpha(q) = \lim_{\varepsilon \to 0} \frac{\sum_{i=1}^{N(\varepsilon)} \mu_i(q,\varepsilon) \lg P_i(q,\varepsilon)}{\lg \varepsilon}, \tag{4}$$

$$f(q) = \lim_{\varepsilon \to 0} \frac{\sum_{i=1}^{N(\varepsilon)} \mu_i(q,\varepsilon) \lg \mu_i(q,\varepsilon)}{\lg \varepsilon}, \tag{5}$$

$$\text{where} \quad \mu_i(q,\varepsilon) = \frac{P_i(\varepsilon)^q}{\sum_{i=1}^{N(\varepsilon)} P_i(\varepsilon)^q}, \tag{6}$$

where $\mu_i(q, \varepsilon)$ is the probability of q at the subinterval i; and $\alpha(q)$ is the singularity exponent. $\alpha(q)$ and $f(q)$ were calculated by using Equations 4 and 5. Multifractal spectrum width $\Delta\alpha$ (α_{max}–α_{min}) can reflect the overall variability in spatial distribution. Δf, $f(\alpha_{min})$–$f(\alpha_{max})$, reflects the multifractal spectrum shape feature and it characterized the degree of symmetry for SPP. $\Delta f<0$ shows that a subset is dominant with a small probability and $f(q)$ has a form similar to that of a hook to the right. In contrast, $\Delta f>0$ denotes that a subset is dominant with a large probability and $f(q)$ has a form similar to a hook to the left (Morató et al., 2017).

2.5 Statistical analysis

The values calculated for SPP, i.e., D_1, ΔD, $\Delta\alpha$ and Δf, were evaluated using statistical methods. SPSS v23.0 (IBM, Inc., Armonk, NY, USA) was used to determine the mean, coefficient of variation (CV) and standard deviation (SD). Least significant difference (LSD) tests were significant at $P<0.05$ level. CV was ranked into three levels that were smaller (<10%), middle (10%–100%) and greater (>100%). Graphs were prepared using Origin Pro v8.0 (OriginLab, Northampton, MA, USA).

3 Results

3.1 Descriptive statistics of SPP

Table 1 showed the mean values, CV and significant difference of SPP in 0–20 cm and 20–40 cm soil layers under three modes of land restoration. The order of clay contents was ML>AL>NR in the whole layer of soil ($P<0.05$), and sand contents were ML<AL<NR ($P<0.05$). CVs of clay, silt content and sand were all lower than <0.10 in the whole soil layer, indicating a low variability.

Table 1 Soil bulk density (BD), field capacity (FC), saturated hydraulic conductivity (K_s) and soil texture (clay, silt and sand contents) in three plots

Soil property	Soil depth (cm)	ML	CV	AL	CV	NR	CV
Clay content (%)	0–20	9.85 ± 0.34^{Aa}	0.03	9.62 ± 0.36^{Aab}	0.04	9.49 ± 0.36^{Ab}	0.04
	20–40	9.99 ± 0.32^{Aa}	0.03	9.72 ± 0.31^{Ab}	0.03	9.61 ± 0.36^{Ab}	0.04
Silt content (%)	0–20	39.20 ± 1.72^{Aa}	0.04	39.33 ± 1.74^{Aa}	0.04	38.61 ± 1.82^{Aa}	0.05
	20–40	40.04 ± 1.71^{Aa}	0.04	39.36 ± 1.7^{Aa}	0.04	38.97 ± 1.70^{Aa}	0.04
Sand content (%)	0–20	50.95 ± 1.61^{Aa}	0.03	51.06 ± 1.57^{Aa}	0.03	51.89 ± 1.69^{Aa}	0.03
	20–40	49.97 ± 1.69^{Ab}	0.03	50.92 ± 1.68^{Ab}	0.03	51.42 ± 1.68^{Aa}	0.03
BD (g/cm^3)	0–20	1.06 ± 0.08^{Bc}	0.07	1.31 ± 0.07^{Bb}	0.05	1.52 ± 0.07^{Aa}	0.05
	20–40	1.25 ± 0.09^{Ac}	0.07	1.49 ± 0.11^{Ab}	0.07	1.55 ± 0.12^{Aa}	0.08
FC (%)	0–20	24.26 ± 0.81^{Aa}	0.03	21.44 ± 1.29^{Ab}	0.06	19.48 ± 1.58^{Ac}	0.08
	20–40	23.21 ± 0.72^{Ba}	0.03	20.08 ± 1.10^{Bb}	0.05	18.91 ± 1.49^{Ac}	0.08
K_s (cm/min)	0–20	0.62 ± 0.13^{Aa}	0.20	0.47 ± 0.24^{Aab}	0.50	0.35 ± 0.25^{Ab}	0.71
	20–40	0.39 ± 0.17^{Ba}	0.44	0.20 ± 0.12^{Bb}	0.58	0.16 ± 0.16^{Bb}	0.99

Note: ML, maize land; AL, alfalfa land; NR, natural recovery land; CV, coefficient of variation. Different uppercase letters within the same plot indicate significant differences between depths at $P<0.05$ level. Different lowercase letters within the same depth indicate significant differences among plots at $P<0.05$ level. Mean±SD.

chinaXiv:202201.00026v1

ChinaXiv合作期刊

In the whole soil layer, BD of NR were 32.9% and 9.6% and significantly higher than those of ML and AL, respectively (P<0.05). FC of ML were 14.3% and 23.7% and significantly higher than those of AL and NR, respectively (P<0.05). K_s of ML were 50.7% and 98.0% and significantly higher than those of AL and NR, respectively (P<0.05). BD and FC of all the land restoration modes had a low degree of variability over the whole soil layer. K_s of ML had a middle variability in 0–20 cm soil layer, while the others were highly variable.

3.2 Multifractal analysis of SPP

3.2.1 Generalized dimension of spatial distribution

Generalized dimension spectra of SPP in 0–20 cm and 20–40 cm soil layers under ML, AL and NR are shown in Figures 3 and 4. D_q values inversely decreased with q values as shown in the spectra "S" shape curve, which indicate that the variables have multifractal characteristics. In this study, SPP having multifractal characteristics implied that multifractal evaluation could be applied.

Table 2 shows the multifractal parameters of SPP. As for the soil texture, D_1 showed the

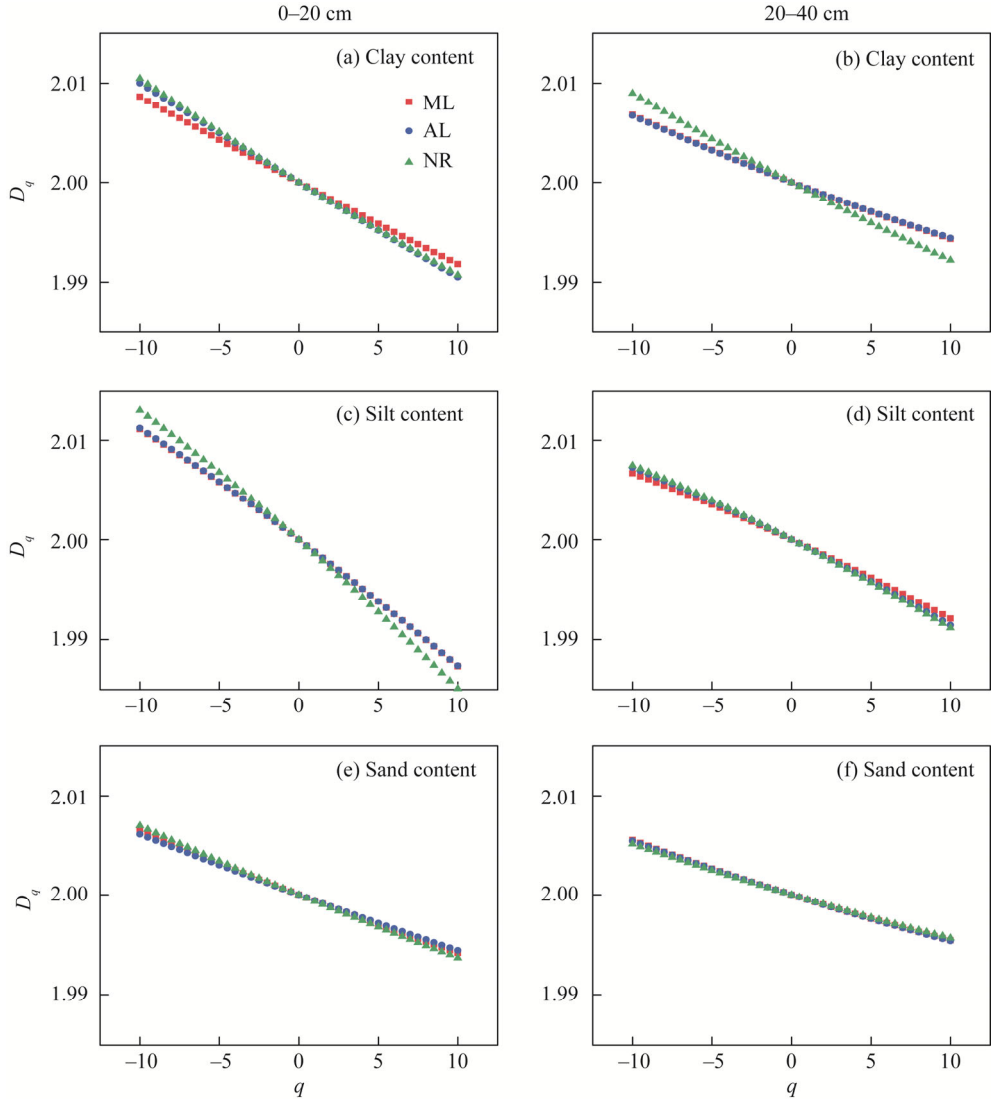

Fig. 3 Generalized fractal dimension (D_q) of soil texture (clay (a and b), silt (c and d) and sand contents (e and f)) in different soil layers in three plots. q, probability density weight index; ML, maize land; AL, alfalfa land; NR, natural recovery land.

chinaXiv:202201.00026v1

ChinaXiv合作期刊

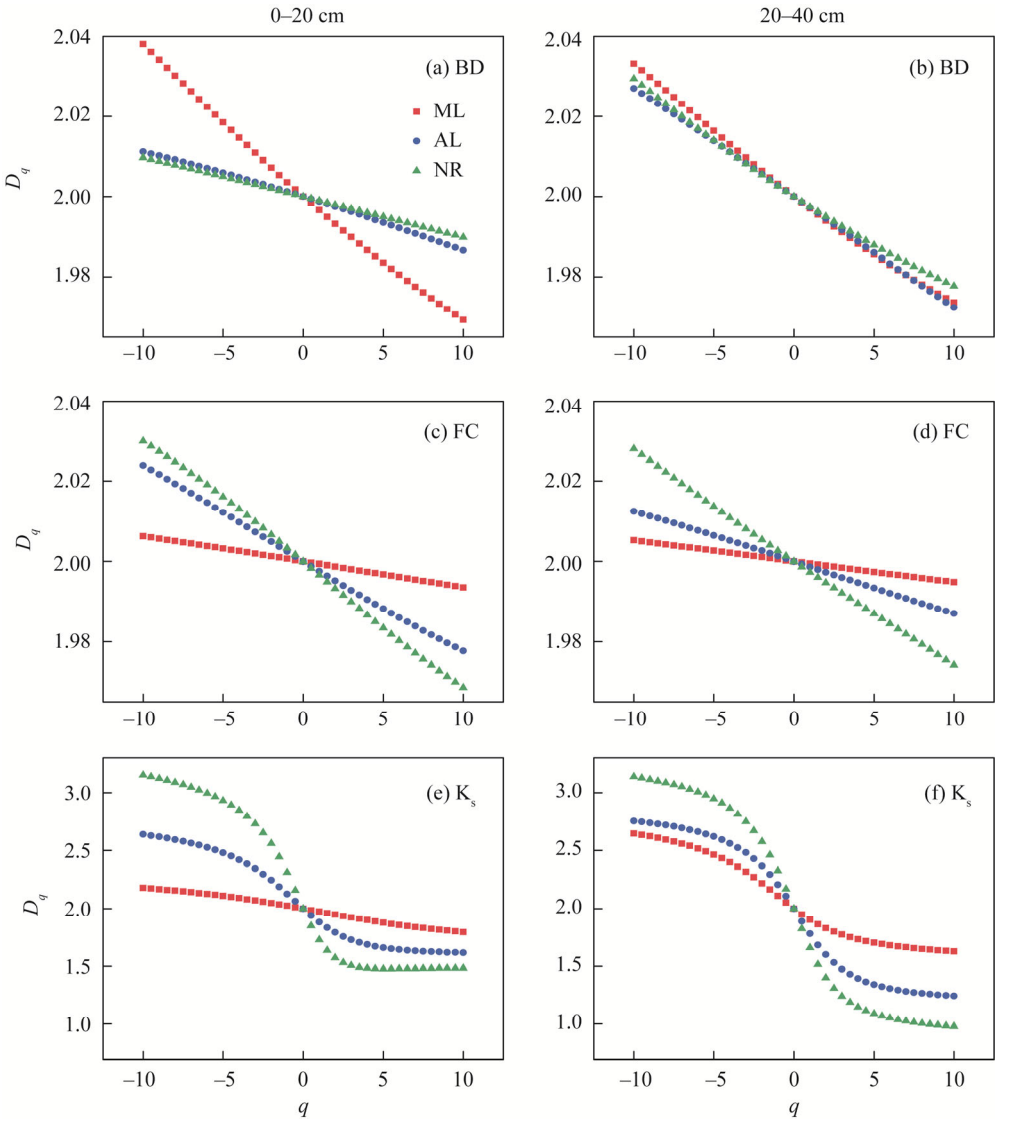

Fig. 4 Generalized fractal dimension (D_q) of soil bulk density (BD; a and b), field capacity (FC; c and d) and saturated hydraulic conductivity (K_s; e and f) in different soil layers in three plots. q, probability density weight index; ML, maize land; AL, alfalfa land; NR, natural recovery land.

tendency of ML≥AL≥NR over the whole soil layer and whatever clay, silt and sand contents are. D_1 values were higher in 20–40 cm layer than in 0–20 cm layer under the same mode, and vice versus for ΔD. For BD, D_1 showed the tendency of ML<AL<NR over the whole layer of soil, while ΔD was ML>AL>NR. For FC and K_s, D_1 and ΔD showed the similar tendency with soil texture in different land restoration modes. D_1 value was higher in 20−40 cm layer than in 0–20 cm in FC, which was opposite for K_s. ΔD was lower in 20–40 cm layer than in 0–20 cm in FC, which was opposite for K_s.

3.2.2 Singularity spectra of SPP

The singularity spectra of SPP was shown in Figures 5 and 6. $\Delta\alpha$ values of clay, silt and sand were higher in 0–20 cm layer than in 20–40 cm soil layer under all the land restoration modes. For BD, $\Delta\alpha$ showed the tendency of ML>AL>NR in the whole soil layer, which was opposite for FC and K_s. Compared with ML, $\Delta\alpha$ values of NR and AL were 4.9- and 3.0-fold that of FC, respectively, while the comparable values were 1.5- and 2.3-fold that of K_s.

Δf values of clay and sand were greater than 0, whose curve was a left hook under all the land

chinaXiv:202201.00026v1

ChinaXiv合作期刊

Table 2 Multifractal parameters for soil bulk density (BD), field capacity (FC), saturated hydraulic conductivity (K_s) and soil texture (clay, silt and sand contents) in three plots

Soil property	Soil depth (cm)	ML				AL				NR			
		D_1	ΔD	$\Delta\alpha$	Δf	D_1	ΔD	$\Delta\alpha$	Δf	D_1	ΔD	$\Delta\alpha$	Δf
Clay content	0–20	1.9992	0.0169	0.0335	0.0081	1.9990	0.0195	0.0388	0.0091	1.9990	0.0198	0.0395	0.0229
	20–40	1.9994	0.0125	0.0253	0.0225	1.9994	0.0124	0.0249	0.0222	1.9992	0.0168	0.0335	0.0229
	Mean	1.9993	0.0147	0.0294	0.0153	1.9992	0.016	0.0319	0.0157	1.9991	0.0183	0.0365	0.0229
Silt content	0–20	1.9988	0.0238	0.0469	–0.0296	1.9988	0.0238	0.0470	–0.0272	1.9986	0.0279	0.0551	–0.0355
	20–40	1.9993	0.0146	0.0288	–0.0245	1.9992	0.0158	0.0312	–0.0259	1.9992	0.0163	0.0320	–0.0269
	Mean	1.9991	0.0192	0.0379	–0.0271	1.9990	0.0198	0.0391	–0.0266	1.9989	0.0221	0.0436	–0.0312
Sand content	0–20	1.9994	0.0122	0.0245	0.0111	1.9994	0.0117	0.0235	0.0103	1.9993	0.0133	0.0267	0.0129
	20–40	1.9995	0.0101	0.0204	0.0187	1.9995	0.0101	0.0203	0.0163	1.9995	0.0095	0.0190	0.0154
	Mean	1.9995	0.0112	0.0225	0.0149	1.9995	0.0109	0.0219	0.0133	1.9994	0.0114	0.0229	0.0142
BD	0–20	1.9965	0.0688	0.1356	0.1243	1.9987	0.0246	0.0476	–0.0440	1.9990	0.0199	0.0390	–0.0096
	20–40	1.9969	0.0596	0.1150	0.1126	1.9972	0.0546	0.1066	–0.0138	1.9974	0.0518	0.1036	0.1345
	Mean	1.9967	0.0642	0.1253	0.1185	1.9980	0.0396	0.0771	–0.0289	1.9982	0.0359	0.0713	0.0625
FC	0–20	1.9994	0.0126	0.0249	–0.0041	1.9976	0.0462	0.0890	0.0256	1.9967	0.0614	0.1134	–0.0257
	20–40	1.9995	0.0103	0.0204	0.0018	1.9987	0.0253	0.0488	–0.0119	1.9974	0.0539	0.1096	0.0338
	Mean	1.9995	0.0115	0.0227	–0.0012	1.9982	0.0358	0.0689	0.0069	1.9971	0.0577	0.1115	0.0041
K_s	0–20	1.9745	0.3820	0.6086	–0.2603	1.8837	1.0203	1.2591	0.7595	1.7287	1.6684	1.9590	1.3434
	20–40	1.9047	1.0157	1.3356	0.5495	1.7815	1.5097	1.7385	–0.7527	1.6603	2.1597	2.4938	–0.7405
	Mean	1.9396	0.6989	0.9721	0.1446	1.8326	1.2650	1.4988	0.0034	1.6945	1.9141	2.2264	0.3015

Note: D_1, information dimension; ΔD, $D_{-10}-D_{10}$, spatial variability in a local distribution; $\Delta\alpha$, $\alpha_{max}-\alpha_{min}$, spatial variability in an overall distribution; Δf, $f(\alpha_{min})-f(\alpha_{max})$, multifractal spectrum shape feature; ML, maize land; AL, alfalfa land; NR, natural recovery land.

restoration modes, whereas silt was a right hook (Fig. 5). For BD, the spectral shapes of AL and NR revealed a right hook in contrast to ML in 0–20 cm soil layer, and the spectral shapes of ML and NR revealed a right hook in contrast to AL in 20–40 cm soil layer (Fig. 6). For FC, spectral shape of ML and NR revealed a right hook and AL revealed a left hook in 0–20 cm soil layer in contrasted to 20–40 cm soil layer. For K_s, the spectral shapes of ML, AL and NR revealed a left hook in the whole soil layer.

4 Discussion

4.1 Effects of land restoration modes on SPP

The homogeneity of SPP seriously affects soil moisture and nutrient distribution, which is an important consideration in farmland management (He et al., 2019). A poor soil structure and a high spatial variability of soil properties after land consolidation have been reported by Chen et al. (2015, 2019). Therefore, many land restoration modes were used to ameliorate soil properties to facilitate crop growth and increase yield (Lozano-Baez et al., 2019; Dou et al., 2020; Šípek et al., 2020).

In our study, the composition of soil texture changed slightly, and BD, FC and K_s were significantly different under the three modes after 5 years of land restoration (Table 1). We found that the spatial variabilities of soil texture were higher in 0–20 cm soil layer than in 20−40 cm soil layer under all the land restoration modes. Moreover, the contents of clay and silt were higher in 0–20 cm soil layer than in 20–40 cm soil layer, in contrast to sand content (Table 2). These results indicated that the content of small size of soil particles increased, while the distribution uniformity decreased in 0–20 cm soil layer. Min et al. (2017) investigated PSD in reclaimed soil produced by mechanical compaction and found that soil particle sizes became finer with the number of compactions. In our study, surface soil was compacted and leveled several times

chinaXiv:202201.00026v1

ChinaXiv合作期刊

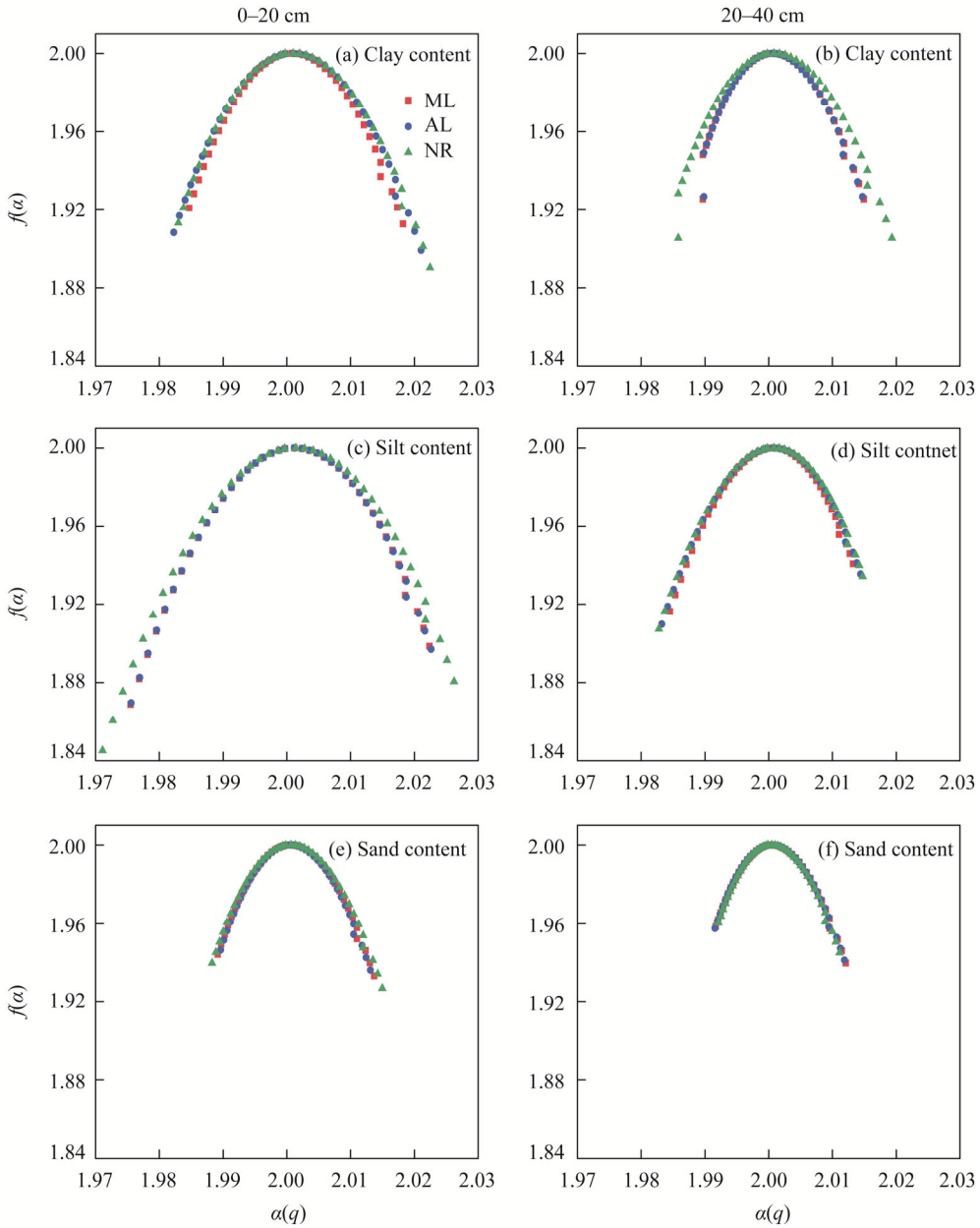

Fig. 5 Multifractal spectrum functions for soil texture (clay (a and b), silt (c and d) and sand contents (e and f)) in different soil layers in three plots. $f(\alpha)$, singularity spectrum; $\alpha(q)$, singularity exponent; ML, maize land; AL, alfalfa land; NR, natural recovery land.

during the formation of excavated farmland, suggesting that a large part of soil particles changed into fine particles and increased the spatial variability of soil texture in 0–20 cm soil layer. Moreover, there were significant differences in the compositions of soil texture under different land restoration modes (Table 1). A difference in the vegetation cover can be a possible primary reason. Qi et al. (2018) have shown that soils in oak forestland, shrub grass sloping land, terraced farmland and sloping farmland were classified as silty loam, sandy loam, sandy loam and loamy sand, respectively, in the Funiu mountainous region, China. Liu et al. (2009) have also shown considerable differences in PSD among seven plant communities in the Yimeng Mountain, China. Another reason of the changes in soil texture could be the frequency of mechanical disturbance.

chinaXiv:202201.00026v1

ChinaXiv合作期刊

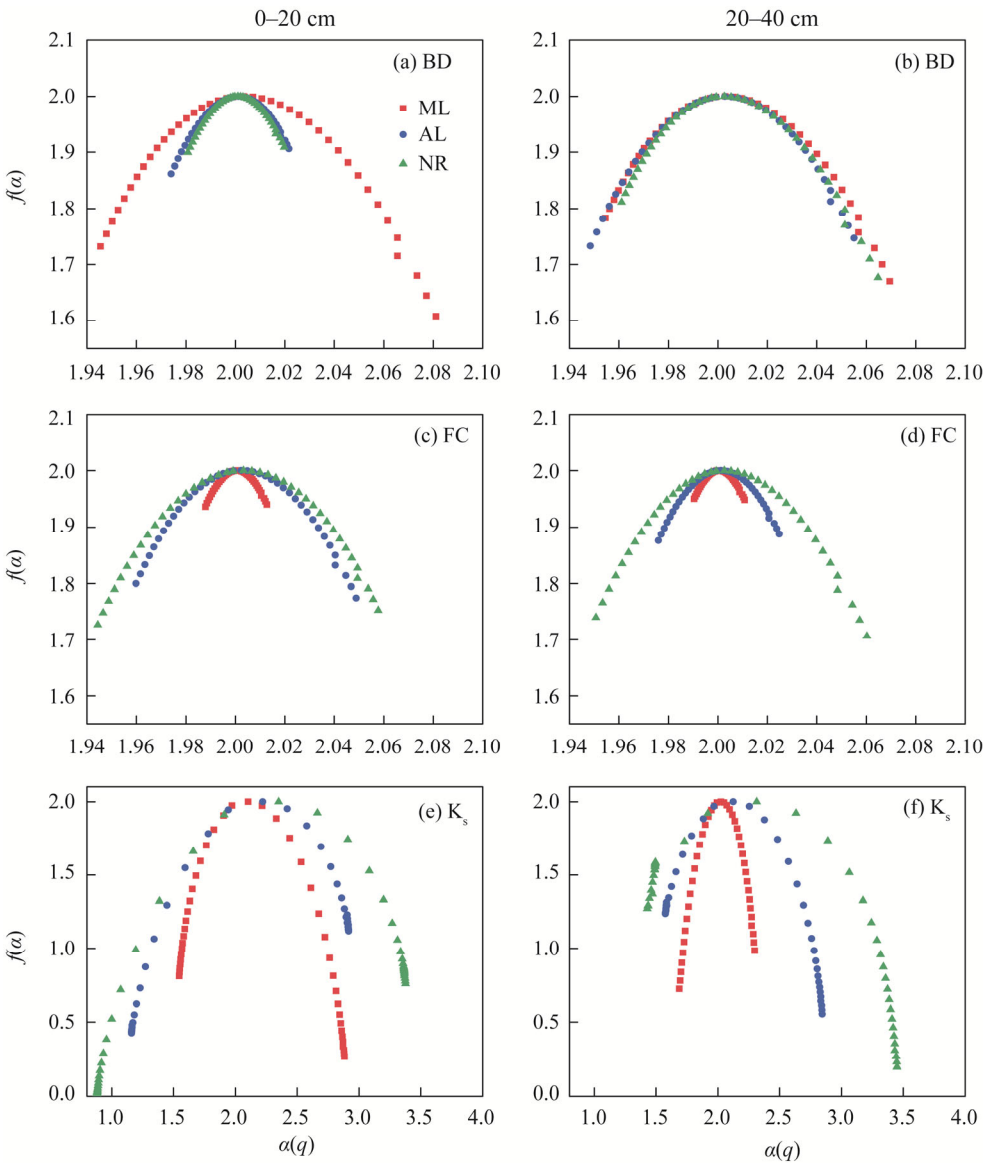

Fig. 6 Multifractal spectrum functions for soil bulk density (BD; a and b), field capacity (FC; c and d) and saturated hydraulic conductivity (K_s; e and f) in different soil layers in three plots. $f(\alpha)$, singularity spectrum; $\alpha(q)$, singularity exponent; ML, maize land; AL, alfalfa land; NR, natural recovery land.

ML was ploughed and weeded twice during growth season. Forage of AL was mechanically harvested three times a year and once a year before returning green. NR was not disturbed by mechinary. Summary, the frequency of mechanical disturbance was the main factor that influenced the changes in soil particles, which was consistent with the result of Min et al. (2017).

ML showed the most significant impacts on BD, FC and K_s, followed by AL and NR (Tables 1 and 2). There are two explanations that consist of both plough numbers and vegetation root characteristics that help explain this result. (1) Owing to a lack of human disturbance, NR basically maintained the condition in which the soil was relatively uniformly compacted after the farmland creation. However, since AL was ploughed once a year before returning to green, and ML was planted to a season of spring maize, and ploughed and weeded twice during growth season, which indicated that, with the increase in plough times, BD decreased, while FC and K_s increased. Thus, plough times were the primary reason that caused ML to be more significantly

chinaXiv:202201.00026v1

ChinaXiv合作期刊

impacted on BD, FC and K_s than those of AL. (2) Most of vegetation types were annual herbs in NR. Guo et al. (2018) reported that the root density of abandoned land was 1.54 kg/m^3 and their roots were concentrated in 0−10 soil layer after 8 years of natural recovery. Huang et al. (2019) showed that root densities of alfalfa and maize were 13.1 and 6.0 kg/m^3, respectively, and 80% of the roots were concentrated in 0–30 cm soil layer. Soil porosity increased in the area with dense root distribution. Therefore, compared with NR, AL and ML had more significant effects on the values and spatial variability of BD, FC and K_s. Moreover, plough numbers were considered dominant because ML had a better SPP than that of AL. These results implied that SPP can be rapidly improved by increasing plough numbers and planting vegetation types with a high root density after land consolidation. In our study, we found that values of BD, FC and K_s were close to those of sloping farmland and terraces in this area after 5 years of land restoration (Wang et al., 2008), thereby indicating that this mode could allow crops to become as productive as normal. In summary, we conclude that ML is an optimal land restoration mode that results in favorable conditions for the rapid improvement of SPP.

4.2 Application of multifractal analysis in SPP

Spatial variability analysis of SPP plays a significant hypothetical role in understanding the excavation and management of farmland. In this study, we observed that physical characteristics of soil have multifractal characteristics using multifractal analyses and parameters (i.e., D_1, ΔD, $\Delta\alpha$ and Δf), which explained the concentration, local variability, overall variability and distribution symmetry of SPP in detail (Figs. 3–6). Using a traditional statistical analysis, we found that CVs of soil texture compositions, BD and FC were in the range of 0.03–0.08. CVs of both soil layers (0–20 and 20–40 cm) were similar, but that does not mean that their spatial distribution was similar (Table 1). Teng et al. (2017) showed that the spatial autocorrelation of soil organic carbon can be effectively expressed through geostatistical analysis, while description of spatial variation was uneven. Studies have shown that a fractal dimension can only reflect the spatial variation but cannot describe the characteristics of PSD more carefully in various types of vegetation using a single fractal analysis (Liu et al., 2009). Moreover, Liao et al. (2017) also found limitations in studying spatial and temporal patterns of soil water content. These results indicated that a multifractal analysis that could describe spatial variations in more detail and in many dimensions and had a substantial advantage in studying the spatial variation of SPP.

Multifractal analysis was based on autocorrelation that was an inherent characteristic of soil properties (Morató et al., 2017). Qi et al. (2018) and Wang et al. (2018a) showed that multifractal analysis can effectively characterize the traits of distribution of soil particle size. Zhang et al. (2019) analyzed soil moisture and soil particle size on the slope of Loess Plateau using a multifractal analysis and found that there was a close relationship between them. We found that most of studies used multifractal analyses to study natural soil, and few of them studied soil properties after land consolidation. Land consolidation destroys soil structure and substantially reduces spatial autocorrelation of SPP. In addition, Pachepsky and Kravchenko (2004) delineated that this type of soil has no multifractal characteristics in some properties. In our study, ML and AL that had been disturbed by large machinery exhibited good multifractal characteristics, and this was also the case for NR. Jing et al. (2019) showed that SPP in subsidence areas in coal mines had multifractal characteristics, and changes in the effects of soil characteristics between land settlement and land restoration were effectively described by multifractal parameters. Therefore, we concluded that a multifractal analysis can be used to study SPP in more complicated situations.

5 Conclusions

In this study, spatial variability of SPP (sand, clay, silt, BD, FC and K_s) were analyzed, and mechanism of effects of diverse land restoration modes on SPP were illustrated using a multifractal analysis for three land restoration modes (ML, AL and NR) after 5 years in the excavated farmland. The main conclusions are as follows: under all the land restoration modes,

chinaXiv:202201.00026v1

ChinaXiv合作期刊

soil particles had fine grains owing to multiple compactions of large machinery in 0–20 cm soil layer. Plough numbers and vegetation root characteristics showed the most significant impacts on the improvement of SPP. These results indicated that ML exhibited the optimal spatial distribution characteristics of SPP compared with those of AL and NR. In addition, values of BD, FC and K_s for ML were close to those of common farmland in this area after 5 years of land restoration. These results implied that ML was an optimal land restoration mode that resulted in favorable conditions for the rapid improvement of SPP.

Land consolidation destroyed soil structure and substantially reduced spatial autocorrelation of SPP. However, ML, AL and NR still had multifractal characteristics. Moreover, multifractal parameters (i.e., D_1, ΔD, $\Delta\alpha$ and Δf) explained the concentration, local variability, overall variability and distribution symmetry of SPP in detail. Therefore, we concluded that multifractal analysis can be used to study SPP in more complicated situations.

Acknowledgements

The study was funded by the National Key Research and Development Program of China (2017YFD0800502) and the National Natural Science Foundation of China (41671510).

chinaXiv:202201.00026v1

References

Abed G A A, Kouzani A, Gyasi-Agyei Y, et al. 2020. Effects of solarisation on soil thermal-physical properties under different soil treatments: A review. Geoderma, 363: 114137, doi: 10.1016/j.geoderma.2019.114137.

Altes W K, Sang B I. 2011. Promoting rural development through the use of land consolidation: The case of Korea. International Planning Studies, 16(2): 151–167.

Boix-Fayos C, Calvo-Cases A, Imeson A C, et al. 2001. Influence of soil properties on the aggregation of some Mediterranean soils and the use of aggregate size and stability as land degradation indicators. CATENA, 44(1): 47–67.

Caniego F J, Espejo R, Martín M A, et al. 2005. Multifractal scaling of soil spatial variability. Ecological Modelling, 182(3–4): 291–303.

Chen Y P, Luo S M, Li F M, et al. 2015. Proposals on the sustainable development of agriculture in Yan'an gully regions. Journal of Earth Environment 6(5): 265–269.

Chen Y P, Wu J H, Wang H, et al. 2019. Evaluating the soil quality of newly created farmland in the hilly and gully region on the Loess Plateau, China. Journal of Geographical Sciences, 29: 791–802. (in Chinese)

Dong W H, Zhang S, Rao X, et al. 2016. Newly-reclaimed alfalfa forage land improved soil properties comparison to farmland in wheat–maize cropping systems at the margins of oases. Ecological Engineering, 94: 57–64.

Donovan M, Monaghan R. 2021. Impacts of grazing on ground cover, soil physical properties and soil loss via surface erosion: A novel geospatial modelling approach. Journal of Environmental Management, 287: 112206, doi: 10.1016/j.jenvman.2021.112206.

Doran J W, Jones J A, Arshad M A. 1996. Physical tests for monitoring soil quality. Soil Science Society of America Journal, 49: 123–141.

Dou Y X, Yang Y, An S S, et al. 2020. Effects of different vegetation restoration measures on soil aggregate stability and erodibility on the Loess Plateau, China. CATENA, 185: 104294, doi: 10.1016/j.catena.2019.104294.

Drewry J J. 2006. Natural recovery of soil physical properties from treading damage of pastoral soils in New Zealand and Australia: A review. Agriculture, Ecosystems & Environment, 114(2–4): 159–169.

Evertsz C J G, Mandelbrot B B. 1992. Multifractal Measures. Berlin: Springer-Verlag, 984.

Federer C A. 1983. Nitrogen mineralization and nitrification: Depth variation in four New England forest soils. Soil Science Society of America Journal, 47(4): 1008–1014.

Fu D G, Wu X N, Duan C J, et al. 2020. Traits of dominant species and soil properties co-regulate soil microbial communities across land restoration types in a subtropical plateau region of Southwest China. Ecological Engineering, 153: 105897, doi: 10.1016/j.ecoleng.2020.105897.

Gao Z Y, Niu F J, Lin Z J, et al. 2021. Fractal and multifractal analysis of soil particle-size distribution and correlation with soil hydrological properties in active layer of Qinghai–Tibet Plateau, China. CATENA, 203: 105373, doi: 10.1016/j.catena.2021.105373.

Guo M M, Wang W L, Kang H L, et al. 2018. Effect of natural vegetation restoration age on slope soil anti-scourability in gully region of Loess Plateau. Nongye Gongcheng Xuebao/Transactions of the Chinese Society of Agricultural Engineering, 34: 138–146. (in Chinese)

He J N, Shi Y, Yu Z W. 2019. Subsoiling improves soil physical and microbial properties, and increases yield of winter wheat in

ChinaXiv合作期刊

the Huang-Huai-Hai Plain of China. Soil and Tillage Research, 187: 182–193.

Huang Z, Sun L, Liu Y, et al. 2019. Alfalfa planting significantly improved alpine soil water infiltrability in the Qinghai-Tibetan Plateau. Agriculture, Ecosystems & Environment, 285: 106606, doi: 10.1016/j.agee.2019.106606.

Jing Z R, Wang J M, Wang R G, et al. 2019. Using multi-fractal analysis to characterize the variability of soil physical properties in subsided land in coal-mined area. Geoderma, 364, 114054, doi: 10.1016/j.geoderma.2019.114054.

Li Q X, Jia Z Q, Liu T, et al. 2017. Effects of different plantation types on soil properties after vegetation restoration in an alpine sandy land on the Tibetan Plateau, China. Journal of Arid Land, 9: 200–209.

Li X D, Shao M A, Zhao C L, et al. 2019. Spatial variability of soil water content and related factors across the Hexi Corridor of China. Journal of Arid Land, 11: 123–134.

Li Y, Li M, Horton R. 2011. Single and joint multifractal analysis of soil particle size distributions. Pedosphere, 21(1): 75–83.

Li Y, Song Y G, Fitzsimmons K E, et al. 2018. New evidence for the provenance and formation of loess deposits in the Ili River Basin, Arid Central Asia. Aeolian Research, 35: 1–8.

Li Y Y, Shao M A. 2006. Change of soil physical properties under long-term natural vegetation restoration in the Loess Plateau of China. Journal of Arid Environments, 64(1): 77–96.

Liang W J, Wei X. 2020. Relationships between ecosystems above and below ground including forest structure, herb diversity and soil properties in the mountainous area of Northern China. Global Ecology and Conservation, 24: e01228, doi: 10.1016/j.gecco.2020.e01228.

Liao K H, Lai X M, Zhou Z W, et al. 2017. Applying fractal analysis to detect spatio-temporal variability of soil moisture content on two contrasting land use hillslopes. CATENA, 157: 163–172.

Liu X, Zhang G C, Heathman G C, et al. 2009. Fractal features of soil particle-size distribution as affected by plant communities in the forested region of Mountain Yimeng, China. Geoderma, 154(1–2): 123–130.

Lozano-Baez SE, Cooper M, Meli P, et al. 2019. Land restoration by tree planting in the tropics and subtropics improves soil infiltration, but some critical gaps still hinder conclusive results. Forest Ecology and Management, 444: 89–95.

Ma J F, Chen Y P, Wang H J, et al. 2020. Newly created farmland should be artificially ameliorated to sustain agricultural production on the Loess Plateau. Land Degradation & Development, 31(17): 2565–2576.

Marschalko M, Yilmaz I, Bednárik M, et al. 2012. Influence of underground mining activities on the slope deformation genesis: Doubrava Vrchovec, Doubrava Ujala and Staric case studies from Czech Republic. Engineering Geology: 147–148: 37–51.

Mehdi H, Fatemeh A, Marzban F, et al. 2019. Interaction between climate and management on beta diversity components of vegetation in relation to soil properties in arid and semi-arid oak forests, Iran. Journal of Arid Land, 11: 43–57.

Min X Y, Li X J, Li Q C. 2017. Influence of mechanical compaction on reclaimed soil particle size distribution multifractal characteristics. Transactions of the Chinese Society of Agricultural Engineering (Transactions of the CSAE), 33: 274–283. (in Chinese)

Morató M C, Castellanos M T, Bird N R, et al. 2017. Multifractal analysis in soil properties: Spatial signal versus mass distribution. Geoderma, 287: 54–65.

Pachepsky Y A, Kravchenko A N. 2004. Soil Variability Assessment with Fractal Techniques. Florida: CRC Press, 617–638.

Paterson S, Minasny B, McBratney A. 2018. Spatial variability of Australian soil texture: A multiscale analysis. Geoderma, 309: 60–74.

Perring M P, Standish R J, Hulvey K B, et al. 2012. The Ridgefield Multiple Ecosystem Services Experiment: Can restoration of former agricultural land achieve multiple outcomes? Agriculture, Ecosystems & Environment, 163: 14–27.

Premo L S. 2004. Local spatial autocorrelation statistics quantify multi-scale patterns in distributional data: an example from the Maya Lowlands. Journal of Archaeological Science, 31(7): 855–866.

Prévost M. 2004. Predicting soil properties from organic matter content following mechanical site preparation of forest soils. Soil Science Society of America Journal, 68(3): 943–949.

Qi F, Zhang R H, Liu X, et al. 2018. Soil particle size distribution characteristics of different land-use types in the Funiu mountainous region. Soil and Tillage Research, 184: 45–51.

Ren Z P, Zhu L J, Wang B, et al. 2016. Soil hydraulic conductivity as affected by vegetation restoration age on the Loess Plateau, China. Journal of Arid Land, 8: 546–555.

Šípek V, Hnilica J, Vlček L, et al. 2020. Influence of vegetation type and soil properties on soil water dynamics in the Šumava Mountains (Southern Bohemia). Journal of Hydrology, 582: 124285, doi: 10.1016/j.jhydrol.2019.124285.

Stanić F, Tchiguirinskaia I, Versini P A, et al. 2021. A new multifractal-based grain size distribution model. Geoderma, 404: 115294, doi: 10.1016/j.geoderma.2021.115294.

Teng M J, Zeng L X, Xiao W F, et al. 2017. Spatial variability of soil organic carbon in Three Gorges Reservoir area, China. Science of the Total Environment, 599–600: 1308–1316.

chinaXiv:202201.00026v1

ChinaXiv合作期刊

Tripathi N, Singh R S, Singh J S. 2009. Impact of post-mining subsidence on nitrogen transformation in southern tropical dry deciduous forest, India. Environmental Research, 109: 258–266.

Wang J M, Wang P, Qin Q, et al. 2017. The effects of land subsidence and rehabilitation on soil hydraulic properties in a mining area in the Loess Plateau of China. CATENA, 159: 51–59.

Wang J M, Lu X, Feng Y, et al. 2018a. Integrating multi-fractal theory and geo-statistics method to characterize the spatial variability of particle size distribution of mine soils. Geoderma, 317: 39–46.

Wang J M, Qin Q, Guo L L, et al. 2018b. Multi-fractal characteristics of three-dimensional distribution of reconstructed soil pores at opencast coal-mine dump based on high-precision CT scanning. Soil and Tillage Research, 182: 144–152.

Wang M R, Liu H J, Lennartz B. 2021. Small-scale spatial variability of hydro-physical properties of natural and degraded peat soils. Geoderma, 399: 115123, doi: 10.1016/j.geoderma.2021.115123.

Wang Y Q, Zhang X C, Han F P. 2008. Profile variability of soil properties in check dam on the Loess Plateau and its functions. Environmental Science, 29(4): 1020–1026. (in Chinese)

Wu Z L, Deng Y S, Cai C F, et al. 2021. Multifractal analysis on spatial variability of soil particles and nutrients of Benggang in granite hilly region, China. CATENA, 207: 105594, doi: 10.1016/j.catena.2021.105594.

Xia J B, Ren R R, Chen Y P, et al. 2020. Multifractal characteristics of soil particle distribution under different vegetation types in the Yellow River Delta chenier of China. Geoderma, 368: 114311, doi: 10.1016/j.geoderma.2020.114311.

Ying L X, Dong Z J, Wang J, et al. 2020. Rural economic benefits of land consolidation in mountainous and hilly areas of southeast China: Implications for rural development. Journal of Rural Studies, 74: 142–159.

Zhang X, Zhao W W, Wang L X, et al. 2019. Relationship between soil water content and soil particle size on typical slopes of the Loess Plateau during a drought year. Science of the Total Environment, 15(648): 943–954.

Zhou H, Li B G, Lv Y Z, et al. 2010. Multifractal characteristics of soil porestructure under different tillage systems. Acta Pedologica Sinica, 47(6): 1094–1100. (in Chinese)

Zhu X M. 1995. More on land management measures of loess plateau. Journal of Soil and Water Conservation, (1): 4–11. (in Chinese)

chinaXiv:202201.00026v1